SUPPLEMENTAL MATERIAL

Rapid Aldosterone-Mediated Signaling in the DCT Increases Activity of the Thiazide-Sensitive NaCl Cotransporter

Lei Cheng[1], Søren B. Poulsen[1], Qi Wu[1], Cristina Esteva-Font[1], Emma T. B. Olesen[1,2], Li Peng[1], Bjorn Olde[3], Fredrik Leeb-Lundberg[3], Trairak Pisitkun[1,4], Timo Rieg[5], Henrik Dimke[6,7], and Robert A. Fenton[1]

[1] InterPrET Center, Department of Biomedicine, Aarhus University, Aarhus, Denmark,

[2] Department of Biomedical Sciences, Faculty of Health and Medical Sciences, University of Copenhagen, Copenhagen, Denmark

[3] Unit of Drug Target Discovery, Department of Experimental Medical Science, Lund University, Lund, Sweden

[4] Faculty of Medicine, Chulalongkorn University, Bangkok, Thailand

[5] Molecular Pharmacology and Physiology, University of South Florida, Tampa, USA

[6] Department of Cardiovascular and Renal Research, Institute of Molecular Medicine, University of Southern Denmark, Odense, Denmark

[7] Department of Nephrology, Odense University Hospital, Odense, Denmark.

Contents:

1. Supplemental Figures (page 2-13)

2. Supplemental Appendix 1 (page 14-25)

3. Supplemental Tables (Excel files) (page 26)

Supplemental Figures

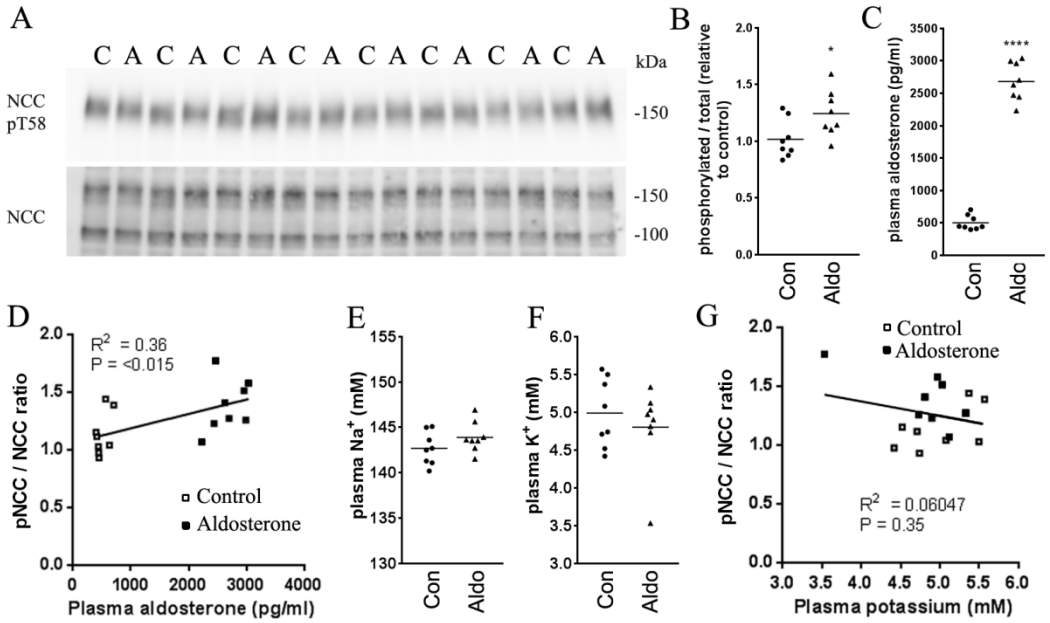

Supplemental Fig. 1. Aldosterone rapidly modulates NCC activity in native DCT cells. A) Mice were injected with aldosterone and after 30 min the phosphorylation levels of NCC at T58 (NCC-pT58, surrogate marker of NCC activation) was assessed by immunoblotting. B) Summary of data (n=8). Data are presented as phosphorylated levels relative to total protein levels and normalized relative to control (Con) conditions. C) Plasma aldosterone levels. D) A significant positive correlation exists between plasma aldosterone concentration and the NCC-pT58/total NCC ratio. E) Plasma Na^+ levels are not significantly different. F) Plasma K^+ levels are not significantly different. G) No significant correlation was observed between plasma K^+ levels and the NCC-pT58 / total NCC ratio after 30 min of aldosterone treatment. *: 0.01<p<0.05; ****: 0.0001<p<0.001.

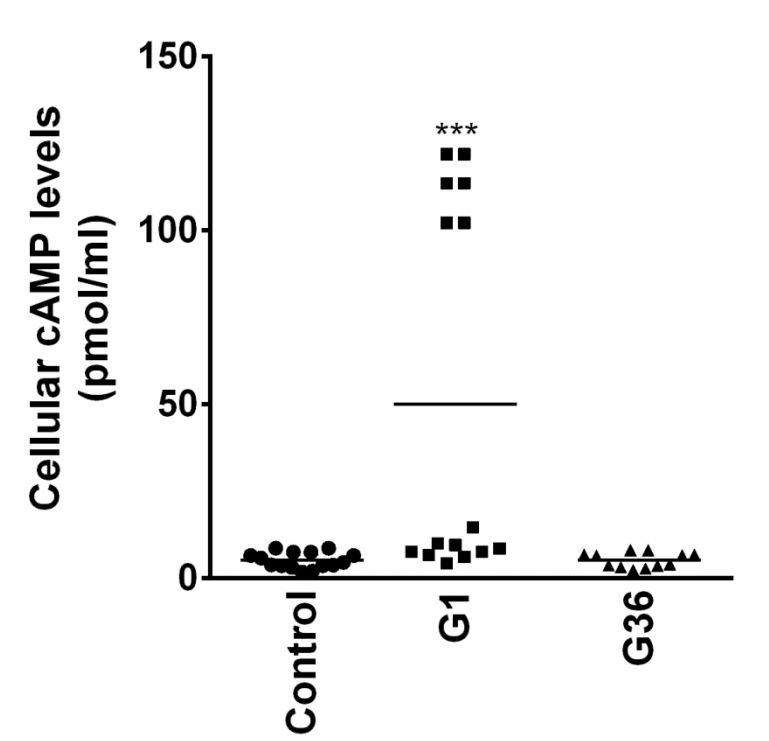

Supplemental Fig. 2. Effects of G-1 and G-36 on cAMP levels in mpkDCT cells. mpkDCT cells were stimulated for 30 min with the GPR30 specific agonist G-1 or the GPR30 antagonist G-36. ***: $0.0001<p<0.001$.

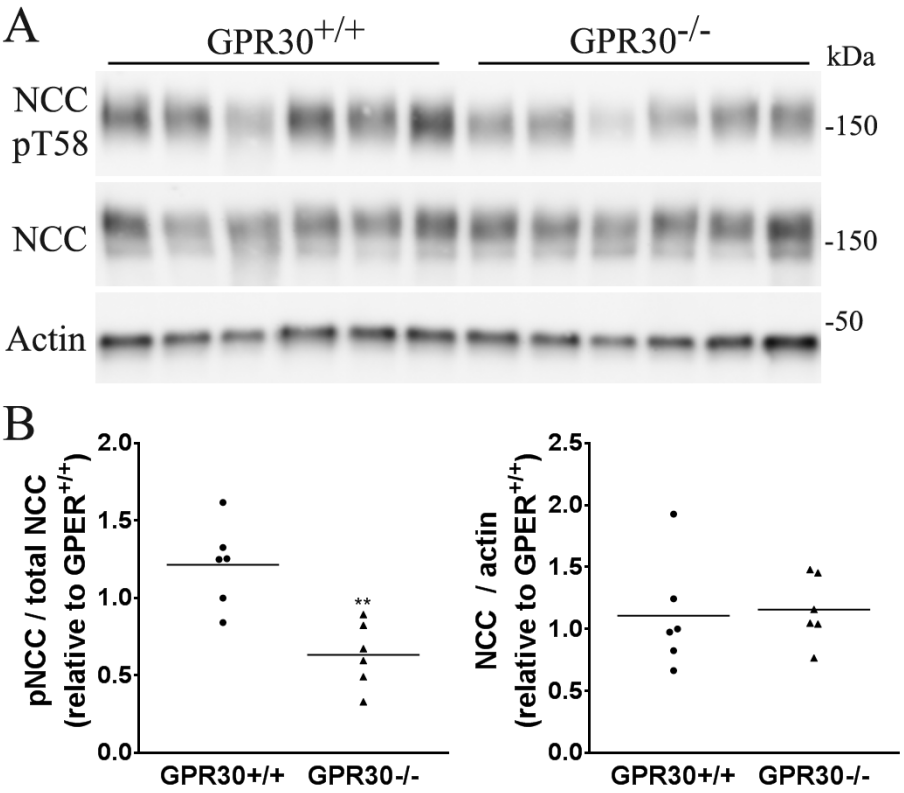

Supplemental Fig.3. Phosphorylated NCC levels are reduced in GPR30 knockout mice. A) NCC levels were assessed by immunoblotting of kidney samples from ovariectomized GPR30$^{-/-}$ and wildtype control mice. B) Summary of data (n=6/group). Data are normalized relative to control conditions. Phosphorylation levels of NCC at T58 (surrogate marker of NCC activation) were significantly reduced in GPR30$^{-/-}$ mice whereas total NCC levels were unchanged. **: 0.001<p<0.01.

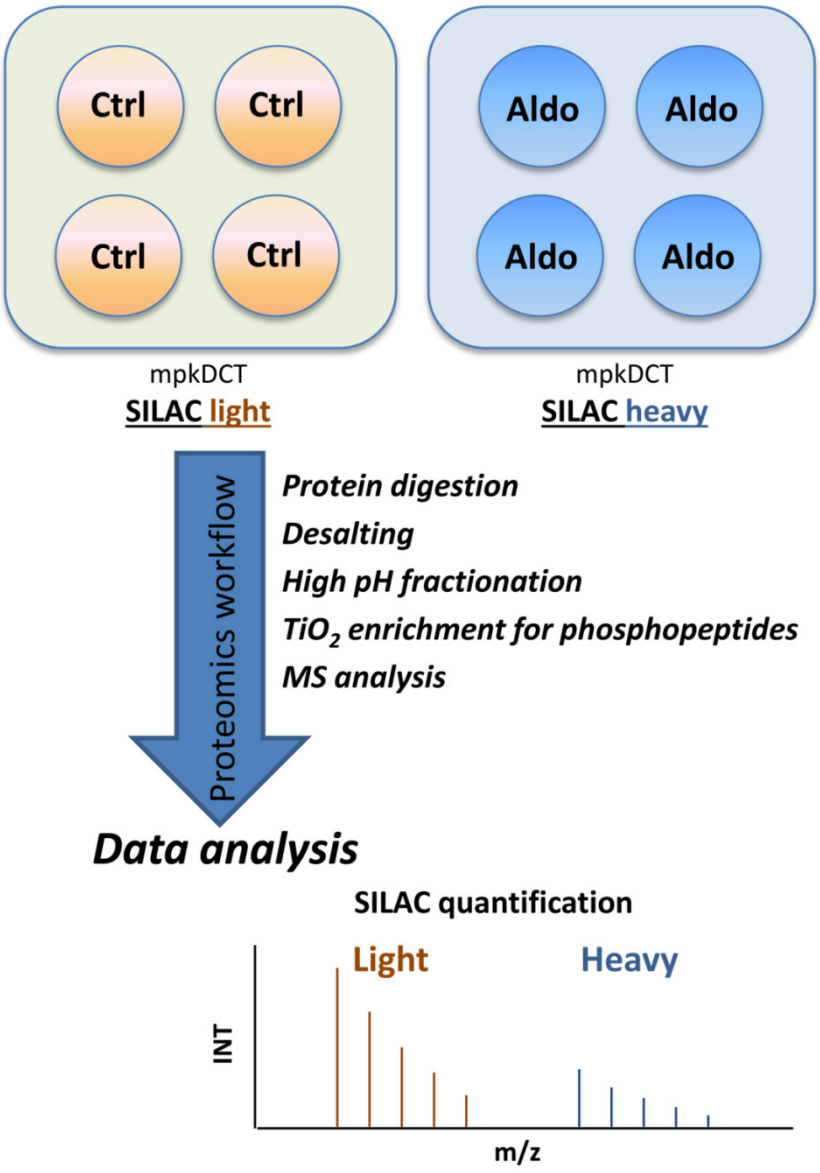

Supplemental Fig. 4. Schematic overview of the experimental phosphoproteomics workflow. Cells were grown in either SILAC light (Lys+0, Arg+0) or heavy media (Lys+6, Arg+10) on filter plates until confluent and stimulated with aldosterone (1nM) for 30 min. Four passages of labelled cells were used to generate four biological replicates for statistical analysis. Cells were harvested, equally pooled and subjected to offline high-pH fractionation based two dimensional LC-MS/MS analysis (Q-Exactive). Peptide quantification was performed at the MS1 level.

A

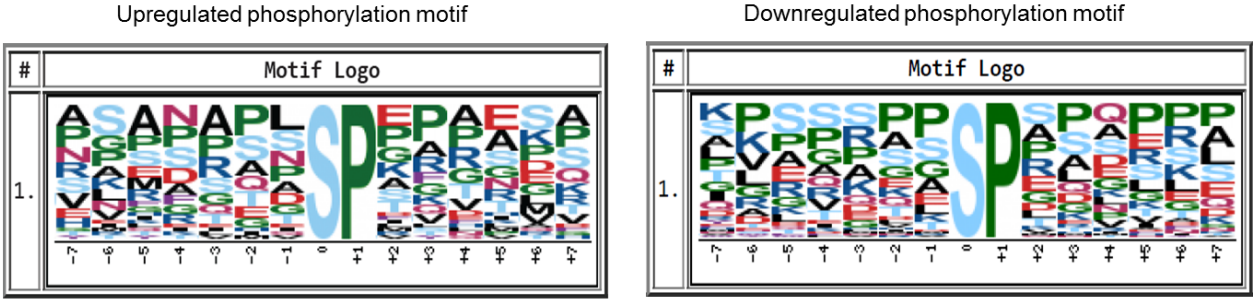

B

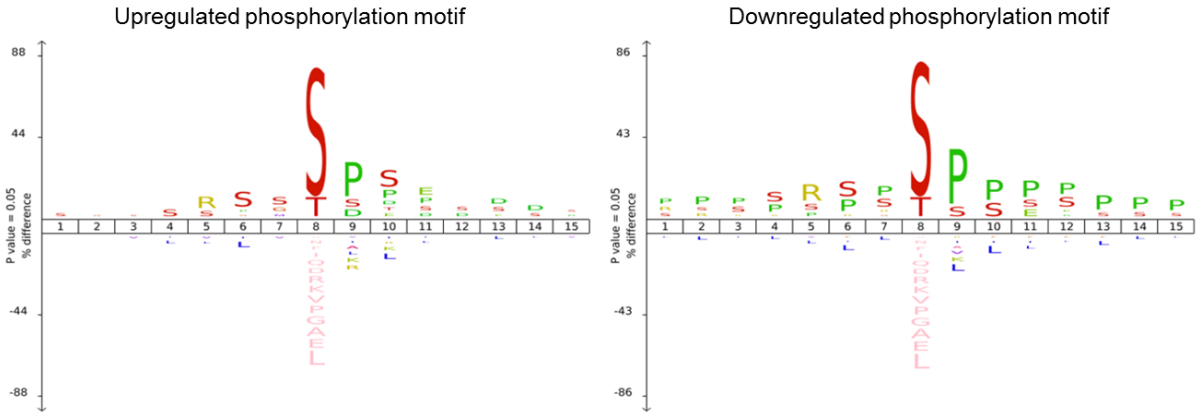

Supplemental Fig. 5. Information based sequence logo of the up- and downregulated phosphorylation motifs following aldosterone stimulation of mpkDCT cells. A) Predicted phosphorylation motifs using Motif-X. B) Predicted phosphorylation motifs using the Icelogo software.

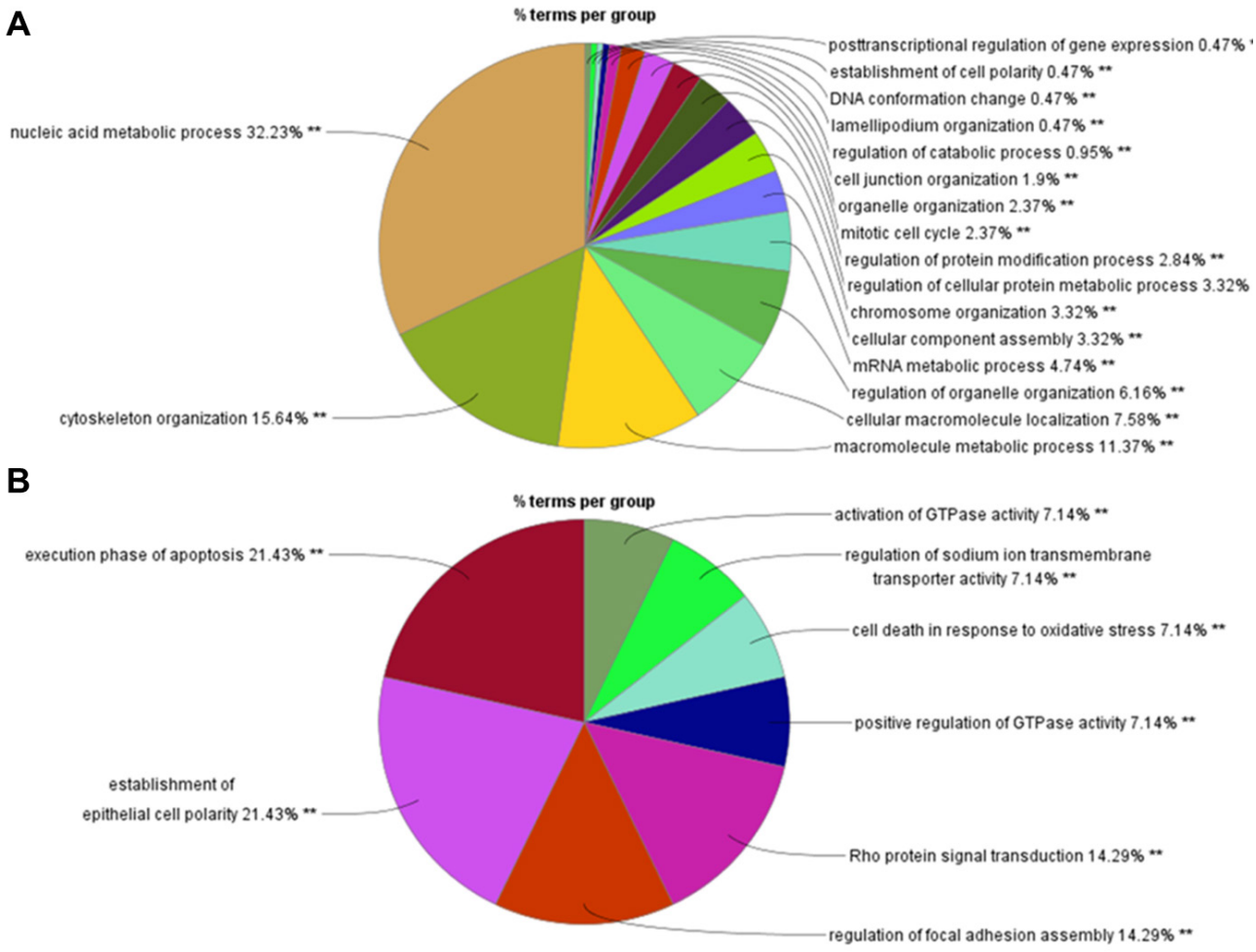

Supplemental Fig. 6. GO-term biological processes analysis by Clue-Go. The terms represent processes that are significantly over-represented in aldosterone regulated genes relative to the whole mouse genome. A) All significantly changed phosphopeptides were included in the analysis. B) Only phosphopeptides with LOG2 ratios higher than 0.5 or lower than -0.5 were included in the analysis. This analysis suggests that aldosterone actions are linked to establishment of epithelial polarity, signal transduction and regulation of sodium ion transmembrane transporter activity. **: 0.001<p<0.01

A

ID	Molecules in Network	Score	Focus Molecul
1	14-3-3, ↑ACACA*, AChR, ↓ACLY*, Aconitase, ↓AFDN*, ↓AHNAK*, ↑AKT2, Alpha catenin, AMPK, ↓ANK3, Ap2 alpha, ↓APC*, ↓ARFGEF2*, ↓ARHGAP35, ↓ATP2B1*, ↓ATXN1, ↓BAG6*, ↓BCOR, ↑C11orf58*, ↑CAD, Cadherin, Calbindin, Calmodulin, CaMKII, ↑CAMSAP3*, ↑CAST*, ↓CCAR2*, ↓CDC42BPB*, CDK4/6, ↑CFL1, ↑CFL2, ↑CGN*, ↓CHD1, Ciap, ↑COBLL1*, Collagen type I, ↑COMT*, ↑CTNNA1*, ↑CTNND1*, ↓CUL4B*, CYP19, cytochrome C, ↓DAP*, ↓DCP1A*, ↑DNAJC5*, ↓DNMT3A, ↑DSTN, ↓DTNB*, ↓EGLN1*, ↑EIF2S2, ↓ERBIN, estrogen receptor, ↓ETV6*, Filamin, ↑FLNC, FSH, ↓GIGYF1*, ↓GIGYF2*, ↓GNL3*, ↓GPN1*, ↓GPRC5A*, Growth hormone, ↑GTF2F1*, ↓HDAC4*, ↓HDAC7*, ↓HDGF*, HDL-cholesterol, IgG1, IgG2a, ↑ITSN2*, ↑KIF13B*, ↑KRT7, ↑KRT18*, Ldh (complex), ↓LEO1, Lh, ↑LMO7*, ↓LRP2, ↑LRRFIP1*, ↑MARCKSL1*, ↓MED1, ↓MIA3*, ↓MTA3, ↑MYCBP2*, N-cor, ↑NCOR2*, ↓NELFB*, Notch, Nr1h, ↑NUMB*, ↓PCDH1*, PEPCK, ↓PGK1, ↓PGRMC1, ↑PHF6, ↑PIAS1, ↑PIK3R2, ↓PKN1*, ↑PKN2*, ↓PKP3*, ↓PKP4*, ↑PLEKHA2*, ↑PLEKHA7, ↑PNN, ↓POLR2A*, ↓PRKRA*, ↑PRPF4B*, ↑PSEN1*, ↑PSIP1*, ↑PSMC3, ↓PSMD1*, ↓PSMD9, ↑PTGES3*, ↑PTPN14, ↑PYGO2, ↑RAB11FIP1*, ↓RALBP1*, ↓RANGAP1*, ↓REST*, Secretase gamma, ↑SIK3, ↓SLC16A1*, ↓SLC6A17, ↓SLC9A3R1*, ↓SNAP23*, Sos, Srebp, ↓SUMO1, ↑SUPT5H, ↑SUPT6H*, ↑TBL1X, ↓TJP2*, ↑TJP3, ↓TOP2B*, ↓UBXN1*, ↓UTRN, ↓XRN2*, ↓YBX3*, ↓ZNF326*	129	109
2	26s Proteasome, ↓ABCC1*, Actin, ↑AKAP12*, Akt, ↑AKT1, ↑AKT1S1, ↑ARMC10, ↓ARVCF*, ATM/ATR, ↓ATRX*, ↓BANF1*, ↑BCLAF1*, BCR (complex), ↑CAMLG, ↓CARHSP1*, caspase, ↑CBX5*, ↓CCNL1*, ↓CDK1*, ↓CEP170B*, ↓CHD4*, ↓CLASP1*, Cyclin A, Cyclin B, Cyclin E, ↑DDX24, E2f, ↓EAF1*, ↑EDC4*, ↑EHMT2, ↓EIF4EBP1*, Eif4g, ↓EIF4G1, ↓ELL, ↓ENSA, ↑EP300*, F Actin, Focal adhesion kinase, ↑FOXK2, ↓GAPDH, Gsk3, ↑GSK3B, ↓HCFC1, Hdac, ↓Hist1h1b*, ↓HIST1H1C, ↓HIST1H1D, HISTONE, Histone h3, Histone h4, ↑HNRNPU*, HP1, ↑HSF1*, Hsp27, Hsp70, Hsp90, ↓HSP90AB1, ↑HSPA8, ↓HSPB1*, ↑IRF2BP1, ↑ISCU*, ↓IWS1*, JINK1/2, ↓KDM1A*, ↓LARP1*, ↓LMNA*, ↓MAPT*, ↑MCM2*, ↓MCM3*, ↓MCM5, ↓MDC1*, ↑MEPCE*, ↓MKI67, MTORC1, MTORC2, ↑NASP, ↑NCL*, ↓NDRG1*, ↑NPM1, ↓NSD2*, P glycoprotein, P-TEFb, p70 S6k, p85 (pik3r), ↑PA2G4, PARP, ↓PCM1, ↓PDLIM5, PI3K (complex), PI3K (family), Pkc(s), ↑POGZ*, PP2A, ↑PPFIBP1*, ↓PPP1CA, ↑PPP1R13L, ↓PRRC2A*, ↓PSMD2, ↓RAD23A*, ↓RAVER1, ↓RBBP6, ↑RBM15*, ↓RBM39, RNA polymerase II, Rnr, RPA, ↑RPS17, ↑RPTOR*, ↑RRM2, ↓SEC61B*, ↓SF3B1*, ↑SHC1*, ↑SMARCAD1*, ↓SMARCC1*, ↓SMARCC2, ↓SMN1/SMN2*, ↓SNW1*, ↓SON*, ↑SP1, ↓SRPK1*, ↑SRSF1, ↓STUB1*, TCR, ↓THRAP3*, ↑TJP1*, ↓TMPO*, ↓TNKS1BP1*, ↓TOM1*, Top2, ↑TP53, ↓TP53BP1*, ↓TRIM28*, ↑TRIM33*, ↓TRIP12, ↑U2AF2, ↓USP39*, Vegf, ↓WDR77, ↓ZMYND8	112	100
3	↓AFF1*, Alpha tubulin, Ap1, ↓AP3D1*, ↓ARAF, ↓ARHGEF7, ↓ARHGEF12*, ↑ARHGEF17, ↓ASAP2, atypical protein kinase C, ↓BCR, ↑BLNK*, Calcineurin protein(s), calpain, ↓CC2D1A, CD3, ↑CD2AP, Cg, ↑CLIP1*, Cofilin, Collagen(s), Creb, ↑CREB1, ↓CTTN*, cytokine, ↓DMTN, ↓DPYSL2*, ↓DYNC1LI1, Dynein, ↓EEF2*, ↓ELF1*, ↓EPB41L1*, ERK, ERK1/2, Fc gamma receptor, Fc receptor, Fcer1, ↓Fmnl1*, G protein alpha, G protein beta gamma, Gm-csf, ↓GRB7, ↓GTF2I*, Hif1, ↑IFIH1*, IFN Beta, Ige, ↓IGF2BP2*, IgG, Igm, IKK (complex), IL1, IL-1R, IL12 (complex), Immunoglobulin, Integrin, Interferon alpha, ↑ITGB4, ↑ITPR1, ↑ITSN1, Jnk, ↓JUND*, ↑KRT8*, LDL, ↓MAP2, ↑MAP4*, ↓MAP1B*, MAP2K1/2, ↑MAP3K1*, ↑MAP3K20*, Mapk, ↑MAPK1*, ↑MAPK3*, Mek, Metalloprotease, Mlc, Mmp, ↑MPRIP, ↓MYO18A*, Nfat (family), ↑NFATC2*, ↓NFKB2, NFkB (complex), NMDA Receptor, ↓NUMA1*, ↑NUP153*, ↓OCLN, ↓P2RY2, P38 MAPK, ↓PAK2, ↑PAK4*, ↑PARD3*, ↓PARVA*, PDGF BB, Pdgfr, ↑PEA15, Pka, Pka catalytic subunit, PLC, ↓PLCB3*, ↑PLEC*, Plk, PP1 protein complex group, ↓PPP1R12A*, Ppp2c, PRKAA, ↑PRKAA1*, ↓PTPN12*, ↓PXN*, Rac, Ras, ↑RERE*, ↑RIPK1, Rock, ↑ROCK1*, Rsk, ↓RTN4*, Ryr, ↑SH3KBP1*, ↑SHANK2, ↓SLC9A1*, ↑SNX1*, ↓SPAG9*, SRC (family), STAT5a/b, ↑STK4, ↑STK24, ↑STRN3, ↑STX7, ↑TBC1D4*, ↑TCF12*, ↑TIAM1, ↓TPR, ↑TRAF2, ↓UNC119*, ↑UNC13D, ↓USP8*, ↓WASHC2A/WASHC2C*, ↑YWHAB, ↓ZC3H14	77	80
4	ABCC4, ACSS1, ↓ADD1*, ↓AEBP2*, AFF4, AGRN, ↓AHNAK*, ↑AKAP12*, amylase, ↓ANK3, ↑ANKRD17*, ↓API5, ↓ARAF, ↑ARHGAP12*, ↓ARHGAP17*, ↑ATXN2, BAP1, ↑BCKDK*, BHLHA15, ↓CARMIL1*, CCNA2, CCNK, CDK9, CHD3, CKS1B, CNBP, CNTNAP2, CSRP2, CST5, CXCL10, CYP26A1, ↑DBN1*, DDX21, ↑DDX46, ↑DOCK9*, DRAP1, E2F8, ↑EDC4*, ↑EEF1A1, EGLN, ↓EGLN1*, EIF2B1, ↑EIF3M, ↑EIF5B*, ↓ELMSAN1*, EPCAM, ↓EPN3*, ERG, EVPL, ↓FAM83G, FGF2, ↓FOXK1*, ↑FTL*, Fus, G3BP1, ↓GAPVD1*, GEMIN7, ↓GPATCH2L*, GTF2F2, ↓HCFC1, ↑HIRIP3*, Hist1h1a, HIST1H1T, ↑HNRNPH1*, ↑IFIH1*, IFNLR1, IGF2BP3, IQGAP2, IRGM, ↑ITPR3*, ↓IVNS1ABP, KMT2E, LAMB3, ↓LARP7*, MAGIL, ↑MFAP1*, ↓MKI67, MLLT3, MYC, ↓MYCBP2*, MYO10, ↓NBEAL2, Nes, NML, ↓NSUN2, ↑NUCB1, ↓NUDC*, ↓NUMA1*, NUP81, ↓PACSIN3, ↓PARVA*, ↓PFKP, ↓PGM1*, ↓PHC3*, ↑PLEC*, ↑PNN, ↓POLA2*, PPP1R10, PPP2R5A, PRKACB, ↑Ptma (includes others), PUF60, ↑RAB11FIP5*, ↓RAPH1*, ↑RBM14, ↑RBMS1, RGS3, RPA1, RPA2, ↓SAFB*, ↑SAMHD1, ↓SCAF11*, SERINC3, SETD1A, ↓SFR1*, SGO1, SH2D5, ↑SLC4A1AP, ↓STAG1*, ↓STAG2*, ↑STK38, SUPT3H, SUZ12, TARDBP, ↑TBC1D10B, THAP1, ↓TICRR, ↓TNS3, ↓TOX4*, TRIM24, ↓TRRAP*, ↓UBE2E3*, UTP18, VARS, ↓WDR33, WDR82, ↓XRN2*, ↓YBX3*, ↑ZC3H4*, ZC3HAV1	68	74
5	ABCC4, ↓ABCF1*, ADRA2B, AGAP2, AKAP8, AKR1B10, ↑AKT1, Alp, AMOTL1, ↓ARHGEF16*, ARID4B, ↑BAIAP2L1*, BARD1, ↓BCR, ↓C2CD2L*, CAMK2N2, CAVIN2, CCND1, ↓CD2BP2, CDCA7, CDCA8, CDCA7L, CDH16, CENPF, ↓CGNL1*, ↑CLNS1A*, CTGF, ↓CXADR*, CYP1A1, DAB2, ↓DIS3L2, ↓DMTN, DNAJA2, ↑DOCK7*, E2F7, E2F8, ↑EEF1A1, EFEMP1, ↓ELF4*, EMILIN1, EMSY, EPCAM, EPHA2, ↓EPPK1*, ERBB2, ↓ERBIN, ERRFI1, EWSR1, F2, FAM103A1, FBXL7, ↓FCHO2*, Fibrinogen, FKHR, FLOT2, GATA1, ↓GATAD2B*, ↓GINS4*, ↓GPALPP1, ↓GRB7, ↓GTF2I*, ↑HDGFL2*, hemoglobin, HIP1, IQGAP2, JAK2, KLHL24, KRAS, ↑KRT7, ↑KRT18*, LEPR, ↓LIG1*, ↓LLGL2*, ↓LMNA*, ↑LRCH4*, LRRC4, MAP2K5, ↑MAP3K1*, ↓MELK*, MS4A2, ↑MYL12B*, ↑MYO9A, MYOC, ↓NCAPD2*, ↓NCAPG*, NCAPH, ↑NEK9*, NFE2, NOX3, ↓NUMA1*, ↓NUP160*, Par6, ↑PARD3*, PARD6G, ↓PARVA*, PCBP2, Pdgf (complex), ↑PDS5B*, ↓PHLDB1, PI3K p85, PLAC1, ↑PLCB3*, ↑PLEC*, ↑PLEKHO2*, ↓PLPP6, ↑PPP1CA, PRKCZ, PRMT1, PRPH, ↓PWP1, QKI, ↑RABL6*, ↑RACK1, RBM38, ↑Rbmxl1*, RFC1, ↑RNMT*, ↑RPRD1B*, ↓SAP130, SLC3A2, SMC2, SMC4, ↑SNRNP70, SOAT1, SOCS2, SOX2, SPTB, ↓SUDS3*, ↑TCEA1, TGM2, TK1, ↑TMPO*, ↑TTLL12, ↓WDR20*, ↑WDR44*, XDH, ↓YBX3*, ↓ZBED5, ↓Zranb2, ZRANB2	55	65
6	↑AAK1*, ↓ABI1, Acp5, AHR, ↓ANKHD1/ANKHD1-EIF4EBP3*, ↓ATP2B1*, ↓ATXN2L*, ↓BCR, ↑BLNK*, ↑BRAP, C1QTNF1, C2CD5, CADM4, ↑CASC3*, Casp12, CBR3, CCL8, CD44, CHST2, CNOT1, COCH, CRABP2, CSNK2B, CTSF, ↓CWC22, Cyb5r3, DARS, ↓DCP1A*, DDX6, ↑DIDO1*, DMBT1, ECSIT, ↑EFTUD2*, EIF4A3, ↓EPB41L2*, ↑EPB41L4A, ↑EPS8L2*, FCMR, ↑FGD4*, ↑Fnbp1l, G3BP1, GLA, GMFG, GRB2, GRM1, H2-M2, HAMP, ↓HDGF*, HELZ, HEXA, HIVEP3, ↑HMGN1*, ↑IFIH1*, IGF2BP3, IPO7, IRGM, JMJD6, KALRN, ↓KLF3*, ↓LARP1*, LAX1, LRPAP1, ↓LSM14A*, ↑LUC7L3, ↓LZTS2, MAGED1, MAGOH, ↑MAP3K1*, ↑MAP3K9*, ↓METTL3*, MS4A2, MTCH2, Muc1, ↑MYBBP1A*, ↓MYO9B, NAGLU, ↓NEDD4L, NFkB (complex), NFKBIE, ↓NOPS6*, NR3C1, ↓NUFIP2*, OTOF, PABPC4, ↓PAK2, PDGF BB, ↓PJA1, PKMYT1, ↓PLCB3*, PTGER4, ↑PTPN12*, ↓PUM2*, ↓RABEP2*, ↑RALGAPA1*, RNA polymerase II, RND3, RNF41, RNU6-1, RPL4, ↑RPL18, ↑RPS17, ↑RPS6KA4*, ↑RPTOR*, RRP8, Sapk, ↓SART3*, ↓SCAF8, SEC61A1, SELL, ↑SGPP1, ↓SIPA1L3*, SIRT1, ↑SLC4A4*, SLC7A1, ↓SLTM*, ↓SMTNL2*, SNRNP200, SOS2, ↓SRP72*, ↓SRRT*, STAT, ↑STK39, ↓STXBP4, ↑SYNPO, TAB3, TAC1, ↓TERF2IP*, ↓TFEB*, TIPARP, ↓TJAP1, TNF, TNFRSF8, TP53I3, TRAIP, TXK, UBA7, WTAP, ↓ZC3H13*, ↓ZC3H18, ↓ZNF395	52	63
7	↓ABLIM1*, ACBD3, ACSS1, ACVR2A, ↓ADD1*, ADGRG2, ↓ADGRL2, ADRB, ↓AEBP2*, ↓AHNAK2*, APOA1, APOM, ARL4C, ↓ASPSCR1*, AVPR1B, ↓BCL9L*, ↑C18orf25*, CADPS, ↑CANX*, ↑CAPZB, CARTPT, ↓CBFB, CD93, CDCA7L, CELSR1, CIAPIN1, Ck2, CNBP, Cng Channel, Crip2, ↑CRTC1, CSDE1, CTNNB1, DCLK1, ↓DDX42, DLEU1, DLEU2, ↓DNAJC21, DPEP1, DSG3, DUSP7, DYNC1H1, E2F7, ↑EEF1A1, ↑EIF3B*, ↑EIF3J*, ↑EP400*, EPHB3, ↑EPN2*, ↑ERC1*, ↓EVL*, Ewsr1, FCGRT, ↓FXR2*, GAA, GALNT6, Gcn5l, GGA3, GLYR1, GPLD1, H2AFZ, HIVEP2, HSD3B7, ↓IGBP1, ↓IGF2R*, IKZF3, IL1R1, IP6K3, IQGAP2, LGMN, ↓LIMD1, LOC100359583/Ptma, ↓LRBA*, ↑MAP4*, ↑MAX, mediator, ↑MFAP1*, ↑MGEA5, MTF2, MTHFD1, MYC, ↑NAV2, ↓NCOA5*, ↑NIPBL, ↓Nolc1, ↓Otud5, ↑PACS1*, PCCA, ↓PDCD4*, ↓PDHA1*, PIAS3, POU3F2, PPAT, ↑PPFIA1, ↑PPP6R3, PRDM5, Proinsulin, ↑PTPN14, ↓PURB*, ↑RAB3IP, RARA, RCC1, ↑RPLP2*, ↑Rplp1 (includes others)*, ↑RPS5, RPS12, SCPEP1, ↑SIPA1L1*, SLC25A19, ↓SLK*, Smad2/3, SMURF2, SOD1, ↑SORBS2, ↓SPTBN1*, ↓SQSTM1*, ↓SSR1*, ↓ST14, SUPT3H, TAF5L, ↓TAX1BP3, ↓TBC1D1*, ↑TCOF1*, thymidine kinase, ↑TLE3*, TLE4, TMEM126A, TOR1A, ↓TOR1AIP1, ↑TRRAP*, TUBB4A, UBA3, ↑UBE2L, ↑UBL7, ↓UHRF1, USP37, WNT16, YWHAG, ↓ZBED6*, ZDHHC6	52	63
8	↑ACE, ACO1, ADAR, AGPAT2, ↑AKAP12*, ↓ANLN*, APP, ↓ARHGAP18*, ARL5B, ↓ARPP19, ↑ATAT1, ATP2A3, ATP6V0C, ↓BCR, ↑BIN1*, BMP6, ↓BYSL, CARTPT, CCNB1, ↑CCNY, CDKN1A, ↓CDV3, CELF1, CENPE, CREB5, ↑CRTC3*, CSNK1E, CTPS1, CTSL, ↑DBN1*, ↓DHX8, ↓DHX16*, DHX58, DRD3, ↓DSP*, ↑DTX3L, Dynamin, DYNC1H1, ↑EIF4G2*, ↓ERBIN, ↓ESYT2*, FRMD6, GAP43, GH2, ↓GPKOW*, GSS, H2AFZ, HELZ2, HIF1A, ↓Hnrnpa1*, HTT, ↓HUWE1*, ID4, IFI44L, IFITM2, IGF2BP3, INSR, Interferon alpha, IRS1, Irs3, ↓KIAA1217*, ↓KLC2, ↓KIF16, KLHL2, ↑KRT20*, LAMP3, LANCL2, LDHC, LDLRAP1, LEP, ↑MAP7*, ↓Marcks*, MBNL1, ↓MCRS1, mGluR, MPEG1, MUS81, Muscarinic cholinergic receptor, MX2, ↓NAB2*, NAPG, ↓NELFA, NME1, ↓NUCKS1, ↑NUMB*, PARP12, ↓PBRM1*, PDE3B, ↓PDHA1*, ↓PEA15, PENK, PER1, Pgk, ↑PHACTR4*, PHLPP2, PIGF, ↑PIK3R2, ↓PKP2, ↑PLEKHG3*, PPARG, ↓PPP1R12C, ↓PPP1R13B*, Presenilin, PRKCA, PRL, ↑PSPC1, ↑RABGAP1, Ras homolog, ↓RBBP6, Rxr, ↑SAMHD1, SIGLEC1, ↓SLBP, SLU7, ↓SLX4*, snRNP, somatostatin receptor, SP110, SPATA18, ST18, ↑STRAP*, SYN2, ↓SYNJ1, ↓SZRD1*, TCF7L2, TDRD7, ↑TNS1*, ↓TRA2A*, ↑TRIM3, TRIM72, ↓TRPV4, ↑TWF1, ↓UHRF1, UQCRC1, ↑USP8*, VHL, YBX2, YY1, ↓ZC3HC1*, ZFP36	48	60
9	↓ACIN1*, ↓AHNAK*, ALDH1A3, AR, ↓ARHGAP32, ARSB, ↓ATAD2*, ATG13, BLZF1, ↓BRD2, BTN2A2, ↑C1orf116, Casp12, Caspase 3/7, ↓CCAR2*, ↓CCDC88A*, Ccl2, CCL25, CCR6, CD160, ↑CDK13*, CHST2, CHST7, Ctf2, Ctla2a/Ctla2b, ↓DGKQ*, DHX58, DPH5, DRD5, DUSP14, EBI3, ↑EBP, ↑EEF1A1, ↓EEF1D*, ↓EIF3G*, ↑EP300*, EVI5, FASTKD2, ↓FNBP1*, FOXI1, Foxo, FYB2, GBP5, Ggt, GIMAP1-GIMAP5, GLG1, ↑GNL1*, GPR34, GPR83, ↑GSK3B, ↓Hist1h1e*, HLA-DMA, HLA-DOA, ↑HNRNPK*, IFI27, IFIT5, IFN81, IFNG, Iga, Igg3, IgG2b, Igh, IKZF3, IL2, IL4, IL7R, ↑IRF2BP1, ↓IRF2BP2, ↓IRF2BPL*, ITPKB, ↑KPNA3, ↓LAD1*, LAG3, LAMTOR2, ↓LMNB1*, Madcam1, ↑MAPK1*, ↑MEX3C*, MMP28, MSH5, MTOR, Muc1, MX2, ↑MYBBP1A*, ↓NAB2*, NCOA3, NFATC2IP, NFKB1, ↓NFKB2, NFKBID, ↓NSD3*, ↓OSBPL3*, OTUD3, PASK, PDGF-DD, ↓PFKFB2, ↓PHF10*, ↑PHLDB2*, ↑PPL*, ↑PPP1R2*, PPP1R17, ↓PPP2R5D*, PRELID1, PRKACB, ↑PRRC2C, PTPN7, ↓RAB12, ↓RB1CC1, RNPS1, RPS13, ↓RREB1*, SAP18, SEC16A, Serpina3g (includes others), ↓Sf1*, SH2D2A, SLC33A1, SP110, ↓Srrm1*, ↑Srrm2*, ↓SRSF11, STAT3, ↓TARS*, TCR, TG, TMEM158, ↑TMF1, TNFAIP8L2, TNFRSF8, TP73, TRAIP, ↓TSPYL1*, Ubiquitin, ULK2, UQCRC1, ↑USO1, VARS, ↑VPS13C*, ↓WFS1*, ↓ZFP91*	40	54

B

Upstream Regulator	Phospho Log Ratio	Phospho p-value	Molecule Type	Predicted Activatio...	Activation z-score	p-value of overlap	Target molecules in ...
Gsk3			group	Inhibited	-2.195	2.48E-03	↓DSP, ↑GSK3B, ↓M.....all 6
IgG			complex	Inhibited	-2.219	1.36E-02	↑AKT1, ↑BLNK, ↑C.....all 5
Plk			group	Inhibited	-2.000	2.87E-02	↓JUND, ↑NFATC2, ↑.....all 4
CYP19A1			enzyme	Inhibited	-2.000	1.50E-01	↑GSK3B, ↑MAPK1, ↑.....all 4
RPTOR	↓-0.211	3.10E-04	other	Inhibited	-2.000	1.54E-02	↑AKT1, ↓EIF4EBP1, ↑.....all 4
Fc gamma receptor			group	Activated	2.000	1.15E-01	↑AKT1, ↑BLNK, ↑... ....all 4
BCR (complex)			complex	Activated	2.131	1.17E-01	↑AKT2, ↑BLNK, ↓... ....all 11
EGFR			kinase	Activated	2.428	2.52E-01	↑GSK3B, ↑ITGB4, ↑... ....all 6
CSF2			cytokine	Activated	2.431	2.63E-02	↑AKT1, ↑AKT2, ↑C.....all 6

EGFR predicted to be activated (z-score 2.428). Overlap p-value **2.52E-01**

6 of 6 genes have measurement direction consistent with activation of EGFR.

ADD TO MY PATHWAY | ADD TO MY LIST | CUSTOMIZE TABLE | CREATE DATASET | More Info

ID	Genes in dataset	Prediction (based on measur...	Phospho Log Ratio	Findings
O89090	SP1	Activated	↑0.360	Increases phosphorylation (2)
P98083	SHC1	Activated	↑0.568	Increases phosphorylation (9)
Q63844	MAPK3	Activated	↑0.585	Increases phosphorylation (7)
P63085	MAPK1	Activated	↑0.585	Increases phosphorylation (9)
A2A863	ITGB4	Activated	↑0.127	Increases phosphorylation (2)
Q9WV60	GSK3B	Activated	↑0.585	Increases phosphorylation (2)

Supplemental Fig. 7. IPA pathway analysis of aldosterone signaling events in mpkDCT cells. mpkDCT cells were treated with aldosterone (1nM) for 30 min and global phosphorylation levels determined using LC-MS/MS. A) IPA core analysis using significantly up or down regulated phosphorylation sites from the phosphoproteomics datasets gave nine complex interlinked networks. B) Upstream regulator analysis of all complex networks highlighted the EGFR to be an activated upstream signaling node.

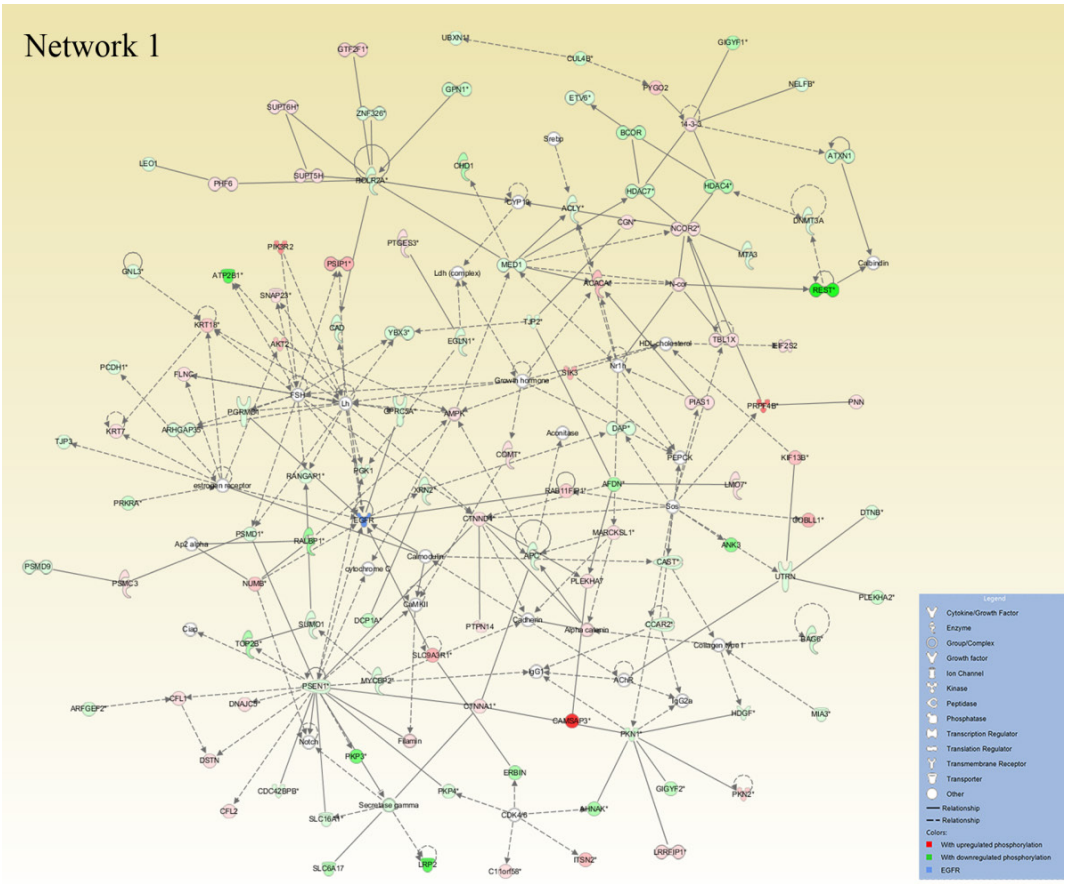

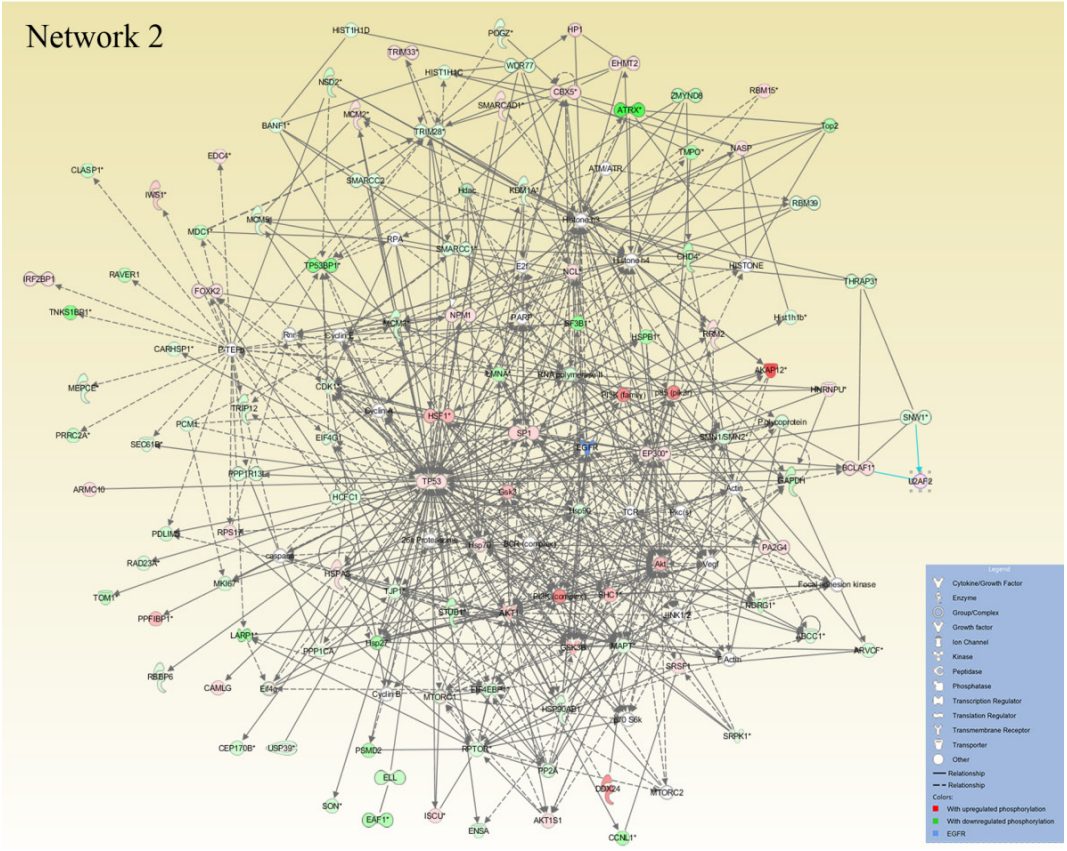

Supplemental Fig. 8. Interaction Network Analysis of the top 4 networks demonstrates that aldosterone stimulation mediates a highly interlinked signaling network. When the EGFR (blue) was added to these networks, it became a central network node connecting key kinases and subsequent

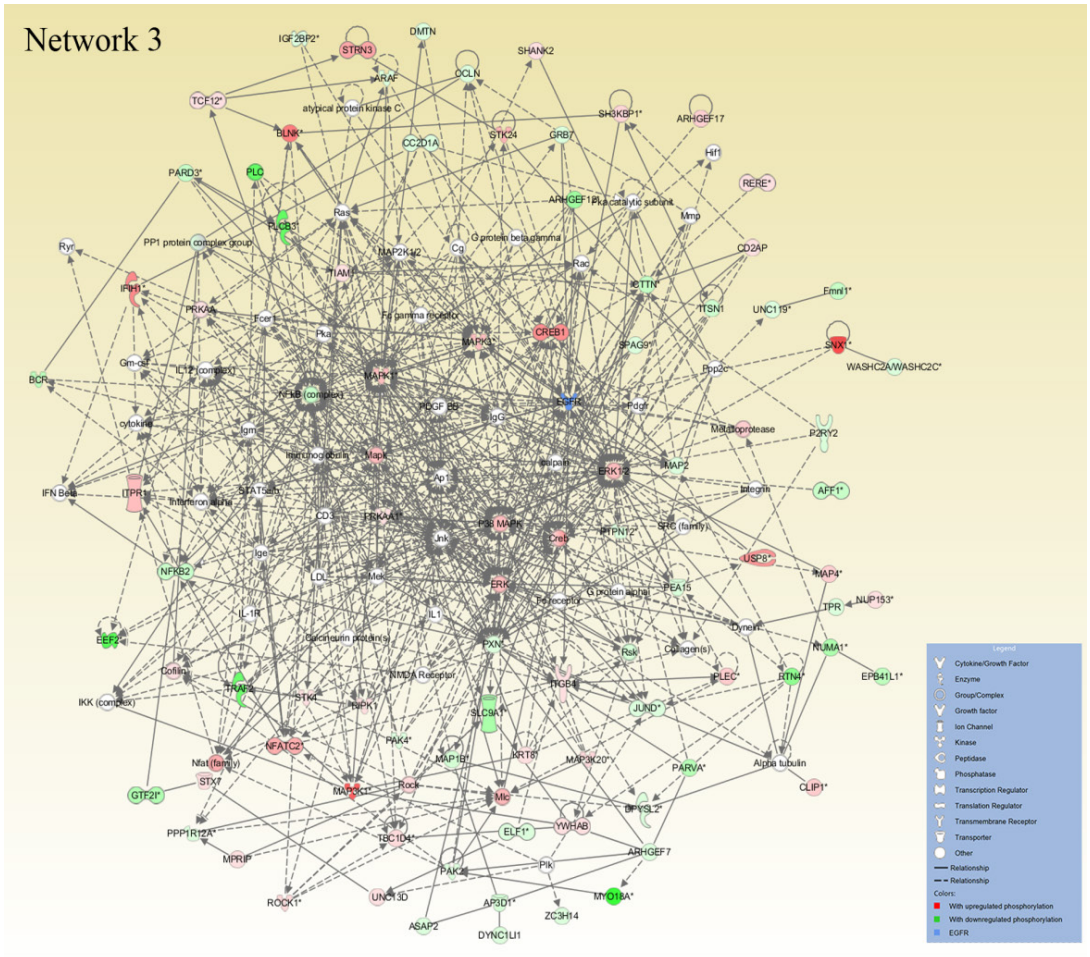

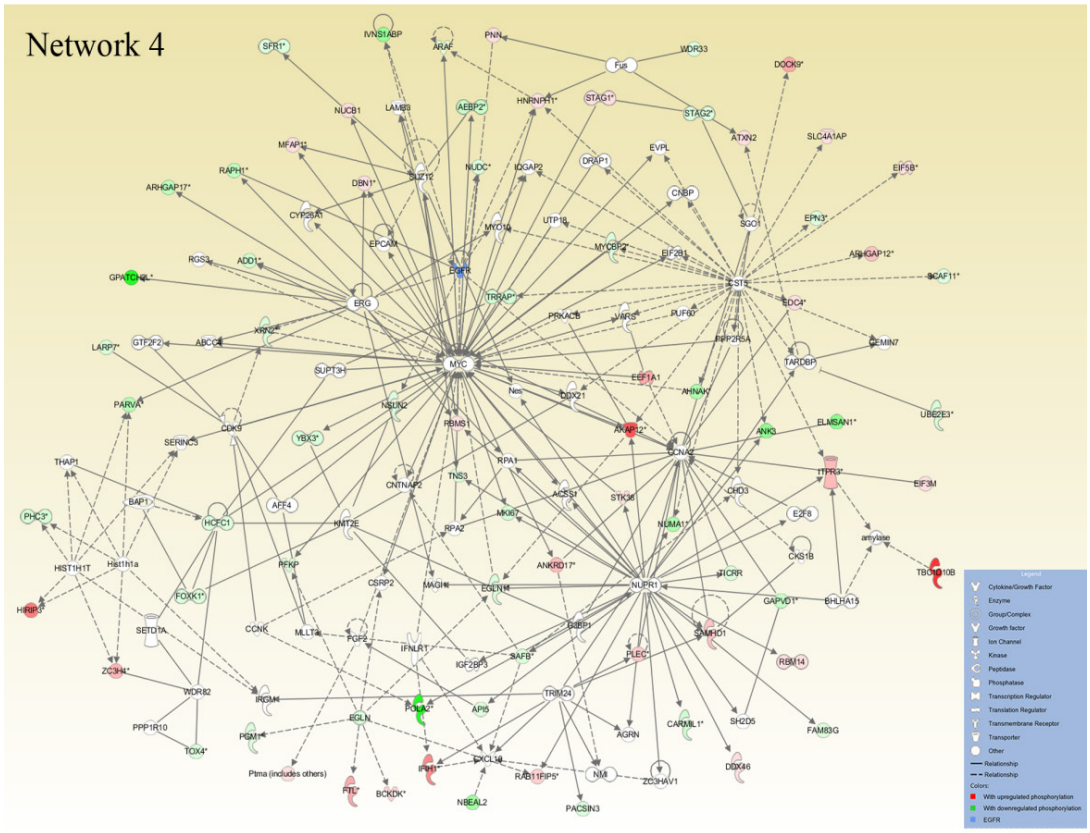

Supplemental Fig. 9. Interaction Network Analysis of the top 4 networks demonstrates that aldosterone stimulation mediates a highly interlinked signaling network. When the EGFR (blue) was added to these networks, it became a central network node connecting key

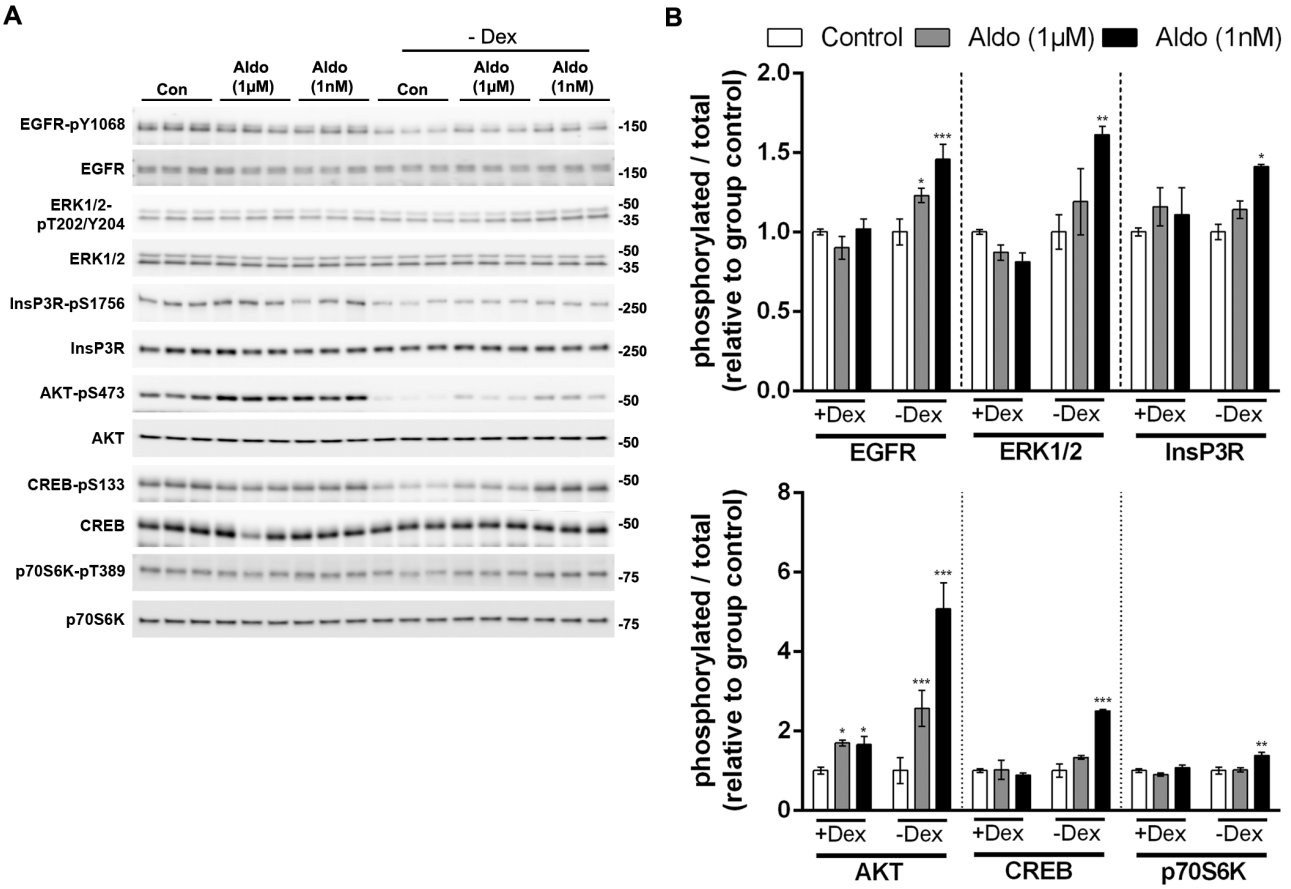

Supplemental Fig. 10. The MR may be involved in the rapid aldosterone mediated transactivation of the EGFR. A) mpkDCT cells were grown in dexamethasone containing media (see methods) and dexamethasone (dex) was removed in some groups for 16h before the experiment. Cells were subsequently treated with aldosterone (1 nM and 10 μM) for 30 min and protein homogenates examined by immunoblotting with antibodies targeting phosphorylation sites of selected proteins. Effects of aldosterone on the EGFR, ERK1/2, InsP3R, CREB and p70S6K were diminished in the presence of dexamethasone. B) Summary of data from 2 independent experiments (n=6/group). Data are presented as phosphorylated levels relative to total protein levels and normalized relative to control conditions. *: 0.01<p<0.05; ***: 0.0001<p<0.001 relative to control conditions.

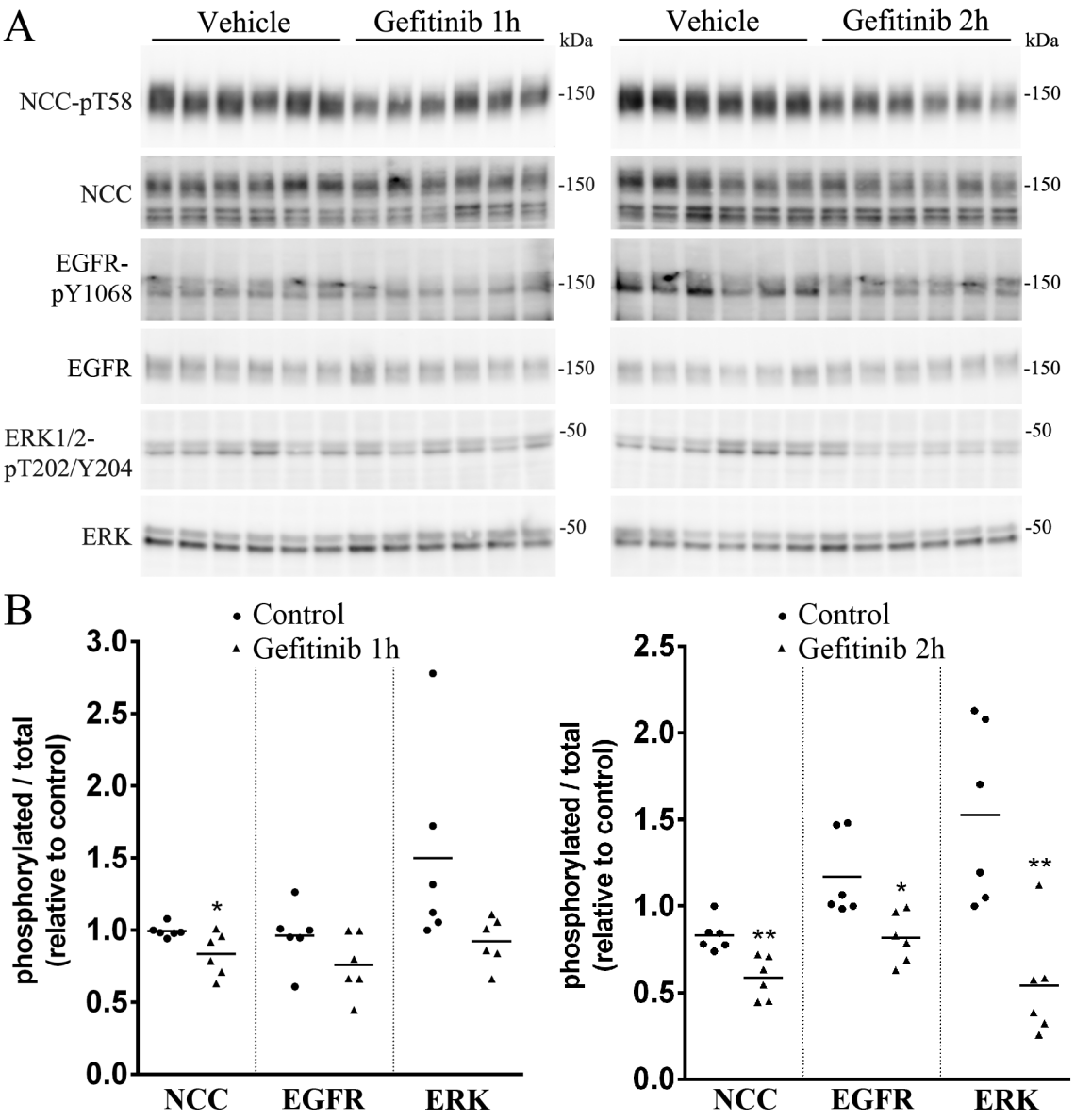

Supplemental Fig.11. Inhibition of the EGFR *in vivo* acutely reduces NCC activity. A) Mice were treated for 1 h or 2 h with either the EGFR antagonist Gefitinib or vehicle and phosphorylation levels of various proteins in the kidney examined by immunoblotting. B) Summary of data (n=6 / group). Data are presented as phosphorylated levels relative to total protein levels and normalized relative to vehicle conditions. *: 0.01<p<0.05; **: 0.001<p<0.01 relative to vehicle group.

Supplemental Appendix 1

Extended methods and materials

Chemicals. G-1 and G-36 (Tocris), aldosterone and ATP (Sigma-Aldrich), and Erlotinib and Gefitinib (Selleckchem) were used at the concentrations as indicated in the text.

Antibodies. The following antibodies were used: SGK1 (Cat # 12103), InsP3R (Cat # 3763), pInsP3R-S1756 (Cat # 3760) CREB (Cat # 9197), pCREB-S133 (Cat # 9198), AKT (Cat # #4685), pAkt-S473 (Cat # 9271), ERK1/2 (Cat # 4695), pERK-T202/Y204 (Cat # 4370), p70S6K (Cat # 9202), p-p70S6K-T389 (Cat # 9234), pPI3K p85-T458 (Cat # 4228), PI3K p85 (Cat # 4257), PDK1 (Cat # 5662), pPDK1-S241 (Cat # 3438), GSK3β (Cat # 12456) and pGSK3β-S9 (Cat # 9323) were from Cell Signaling. EGFR Y1092 (ab40815) and EGFR (ab52894) were from Abcam. pSGK-S422 (sc16745) and GPR30 (sc48524R) were from Santa Cruz. Specificity of the commercial antibodies was based on that they either gave a single unique band on an immunoblot corresponding to the target proteins predicted molecular weight, or the most prominent band on the immunoblot was at the target proteins predicted molecular weight (with no other bands of similar size). Other antibodies were SPAK and pSPAK [1] and pNCC-T58 [1].

Ca^{2+} and cAMP measurements. The mouse kidney DCT cell line (mpkDCT) has been demonstrated to be an excellent model of the DCT [2]. Cells were routinely cultured at 37oC in 5% CO_2 in mpkDCT medium (DMEM/F12- media (Invitrogen) containing 60 nM sodium selenite, 5 µg/ml transferrin, 2 mM glutamine, 1 nM triiodothyronine, 10 ng/ml epidermal

growth factor, 5 µg/ml insulin, 20 mM D-glucose and 20 mM HEPES (pH 7.4)) as previously described [3]. For Ca^{2+} assays, cells were cultured in black Visiplates (Wallac) until confluent, with the last 24 h in pure phenol red free DMEM-F12 media (Invitrogen). Cells were washed with HBSS before incubating in dye loading solution (5 µM Fluo-4, 2.5mM probenecid, 1x PowerLoad in HBSS) for 30 min at 37°C. Cells were washed in assay buffer (HBSS containing 2.5 mM probenecid) and overlaid with 200 µl assay buffer. Fluorescence was measured using an EnSpire plate reader (PerkinElmer), with an excitation wavelength of 495 nm and an emission wavelength of 510 nm continuously for 2 min (background fluorescence) and for 10 min after addition of 50 µl of agonist (to reach final concentrations as indicated) or control solution. For cAMP assay experiments, cells were grown on a semi-permeable filter support (Transwell, Corning) until a fully confluent polarized monolayer was formed (transepithelial resistance (TER) >5 $k\Omega.cm^2$). Cells were stimulated as indicated for 30mins, lysed and intracellular cAMP levels were measured using a cAMP enzyme immunoassay kit (Enzo) according to manufacturer's instructions. All measurements were carried out in triplicates on at least 5 separate days.

Inositol Phosphate (IP) measurements. IP accumulation was measured using a scintillation proximity based inositol-phosphate accumulation assay (SPA-IP [4]). In brief, mpkDCT cells were seeded at 35,000 cells/well in 100 µL mpkDCT medium in 24-well filter plates and incubated for 24 h at 37°C with 0.5 µCi of myo-[^{3}H]inositol (PerkinElmer). Medium without myo-[^{3}H]inositol was added to the basolateral compartment. The following day, cells were washed twice in pure DMEM-F12 (Invitrogen) and incubated in pure DMEM-F12 supplemented with 10 mM LiCl at 37°C for 30 min in the presence of diluent (DMSO), aldosterone (1nM) or the activator of phospholipase C m-3M3FBS (Tocris) as a

positive control. Cells were incubated in 10 mM formic acid for 60 min. 35 µl from each well was transferred to a 96-well plate, 1 mg of yttrium silicate SPA beads (SPA-Ysi; RPNQ, PerkinElmer) added and the plate mixed for 30 min by high-speed agitation. Beads were centrifuged (5 min, 400 g) and [^{3}H]inositol phosphate binding was measured on a TopCount NXT (PerkinElmer, Waltham, MA).

Immunoblotting experiments. mpkDCT cells were grown on filter plates in mpkDCT media until a fully confluent polarized monolayer was formed (TER >5 kΩ.cm^2). The evening prior to experiments, cells were cultured in pure phenol red free DMEM-F12 media (Invitrogen). Cells were treated with agonists/antagonists or relevant control solutions as indicated for 30 min at 37^{o}C. For G-36 antagonist experiments, cells were pre-incubated with G-36 or pure media for 20 min prior to subsequent stimulation. Cells were lysed in Laemmli sample buffer containing DTT (15 mg/mL), sonicated and heated at 65°C for 15 min. Standard procedures were utilized for SDS-PAGE. Immunoblots were developed using ECL detection and signal intensity in specific bands were quantified using Image Studio Lite (Qiagen) densitometry analysis. For detection of GPR30 and EGFR in native DCT cells, purified DCT cells were isolated from parvalbumin-GFP mice as previously described [5].

Immunohistochemistry and confocal microscopy analysis. Archived paraffin-embedded male mouse kidney tissue was processed and immunolabeled for light- or confocal laser scanning microscopy as previously described [6]. Microscopy was carried out with a Leica DMRE light microscope or a Leica TCS SL confocal microscope with an HCX

PL APO 63 x oil objective lens (numerical aperture: 1.40) (Leica Microsystems). Brightness was digitally enhanced on presented images.

Reverse-transcriptase PCR (RT-PCR). RNA purification and RT-PCR was performed on 1 µg RNA as previously described [7] . Archived cDNA from male C57BL/6J mouse kidney cortex was used as a positive control. Primers are; GPR30 forward 5'-CACGTGACATTGACCTCTGACCT and GPR30 reverse 5'-TCACTCAGGAGTTAGGAGTGGCA, EGFR forward 5'-CTTCAAGGATGTGAAGTGTG and EGFR reverse 5'-TGTACGCTTTCGAACAATGT.

Mouse cortical tubule suspensions. Mouse cortical tubule suspensions were prepared as previously described [2]. Equal volumes of the suspensions were plated into 24-well tissue culture plates and pre-incubated in pure DMEM-F12 media (Invitrogen) for 150 min at 37°C / 5% CO_2. For erlotinib and G36 studies, the antagonists were added to the suspensions for the last 30 min of pre-incubation. Suspensions were treated using antagonists, aldosterone (1 nM) or relevant controls as indicated in text for 30 min at 37°C / 5% CO_2. In some studies, 5 µM actinomycin D and 100 µM cycloheximide (Sigma-Aldrich) were included throughout the pre-incubation and stimulation steps. At the end of the experiment media was removed and cells lysed in Laemmli sample buffer containing DTT (15 mg/mL), sonicated and heated at 65°C for 15 min before immunoblotting. For high potassium experiments, KCl was added to the media where indicated to make the final K^+ concentration 8 mM.

***Isolation of Enhanced Green Fluorescent Protein (EGFP) expressing mouse DCT cells*.** All animal protocols comply with the European community guidelines for the use of experimental animals and were approved and performed under a license issued by the Danish Ministry of Justice (Dyreforsøgstilsynet). Mice had free access to standard rodent chow and water. Transgenic mice expressing EGFP driven by the parvalbumin promoter [8] were euthanized by cervical dislocation and kidneys quickly removed. The kidneys were sliced into approximately 1 mm pieces and incubated for 40 min in buffer B (125 mM NaCl, 0.4 mM KH2PO4, 1.6 mM K2HPO4, 1 mM MgSO4, 10 mM Na-acetate, 1 mM α-ketogluterate, 1.3 mM Ca-gluconate, 5 mM glycine, 30 mM glucose and 5 µg/mL DNase I (Sigma), pH 7.4) containing 2 mg/ml collagenase B (Roche). Samples were mixed continuously at 850 rpm at 37°C. After 10 min, half of the enzyme solution was removed and replaced with buffer B without collagenase, and samples were incubated for a further 10 min. This procedure was repeated for another 10 min. After a total incubation of 40 min, the tubular suspensions were passed through a 100 µM cell strainer (BD Falcon), and centrifuged for 3 min at 200 g. Cells were washed with a trypsin/EDTA solution (Lonza) containing 10 mM HEPES, 30 mM glucose and 50 ug/ml DNase I. Cells were again resuspended in trypsin/EDTA solution and incubated for 15 min at 37°C. Cells were washed in DMEM/HamF12 cell culture medium (Gibco) containing 5% FBS, 30 mM glucose, 10 mM HEPES and 50 mg/ml DNase I and subsequently resuspended in 1.5 ml medium. Cells were passed through a 40 µM cell strainer and kept at 4^0C. EGFP-positive and negative cells were isolated on a FACSAria III (BD Biosciences) machine at the FACS Core Facility, Aarhus University, Denmark. Sorted cells were centrifuged for 10 min at 3,000 g at 4^0C and the pellet was resuspended in 1x Laemmli sample buffer (62.5 mM Tris, 8.75% Glycerol, 3% SDS, 89.5 µM Bromphenolblue, 15 mg/ml DTT, pH 6.8).

Samples were heated for 10 min at 65^0C. EGFP purity changed from 4% before sorting to 94% after sorting in the EGFP-positive sample (DCT cells).

Acute aldosterone effects in mice. All animal protocols comply with the European community guidelines for the use of experimental animals and were approved and performed under a license issued by the Danish Ministry of Justice (Dyreforsøgstilsynet). Male C57BL/6J mice (approx. 30 g bodyweight) were administered 50 µl of an aldosterone solution (43 µM in DMSO) by intramuscular injection. This resulted in a 3-fold increase in plasma aldosterone levels as measured using an enzyme immunoassay kit (EIA-5298; DRG International, Springfield, NJ; range 20–1,000 pg/ml; QC: standards) (**Fig. 1**). After 30 or 60 min, animals were anesthetized using isofluorane and blood sampled from the retro-orbital plexus. Kidneys were removed and processed for immunoblotting as previously described [1]. Sodium and potassium levels in the urine were determined using flame photometry (Sherwood Model 420).

***In vivo* role of EGFR**. All animal protocols were approved and performed under a license issued by the Danish Ministry of Justice (Dyreforsøgstilsynet, permit #2014-15-0201-00043). 10 week old male FVB mice (Janvier Labs, France) were used and their bladder emptied at the beginning of the experiment. Mice received either Gefitinib (0.8 mg/g bodyweight, Selleckchem) or vehicle (20% PEG300) by gavage (250 µl). The experimental period was 3 h, during which the mice were housed in their usual cages. Spot urine was collected during the last 1 h period. Blood was removed from vena cava under isoflurane anesthesia into lithium heparin tubes, the animals euthanized and the kidneys collected

and snap frozen in liquid N_2. Immunoblotting samples were prepared as previously described [9]. Creatinine in urine and plasma was determined using a colorimetric assay (ABX Pentra Creatinine 120 CP kit, Horiba ABX SAS, Montpellier, France) according to the manufacturer's instructions. Sodium and potassium levels in the urine were determined using flame photometry (Sherwood Model 420). For study 2, 10 week old female FVB mice (Janvier Labs, France) were used and the experimental period was 1 h or 2 h. For study 3, 10 week old male FVB mice (Janvier Labs, France) were used. After 1 h treatment with Gefitinib or vehicle, mice were administered 50 µl of an aldosterone solution (43 µM Aldosterone) in 3.2 ul DMSO in 1.5 ml saline or vehicle by intramuscular injection. The experiment was terminated 1 h later by decapitation and trunk blood collected.

***In vivo* role of GPR30**. Generation of the GPR30$^{-/-}$ mice has been previously described [10]. Animal care was in accordance with institutional guidelines. Archived kidneys isolated from three-month-old female GPR30$^{-/-}$ and wildtype control mice four weeks after ovariectomy were used [11]. All animal experiments were approved by the Ethics Committees for Animal Research at Gothenberg University and Karolinska Institutet.

SILAC labeling. mpkDCT cells were grown in SILAC advanced DMEM/F12-Flex media (Invitrogen) in light (12C6 lysine, 12C6 14N4 arginine) or heavy (13C6 lysine, 13C6 15N4 arginine) conditions for at least 21 days (3-5 passages). Mass spectrometry (MS) confirmed labeling efficiency >97%. Cells were grown on filter plates until a fully confluent polarized monolayer was formed. On the day of experiment, cells were incubated in phenol red and serum-free pure media for 4 hrs. Aldosterone (1 nM) was added to both

apical and basolateral compartments of experimental group, controls received an equivalent volume of DMSO. After 30 min cells were washed twice in ice-cold PBS and scraped in cell lysis buffer (8 M urea, 2 M thiourea, 50 mM Tris, pH 7.5) containing protease and phosphatase inhibitors (Halt protease and phosphatase inhibitors). After 20 min incubation, lysates were sonicated on ice and centrifuged at 16,000g for 10 min at 4^{o}C. Protein concentrations were determined by BCA assay (Pierce) and equal quantities of differentially labelled control or hormone-treated samples were pooled. In all four generation of DCT cells (S1, S2, S3 and S4), heavy labelled cells were treated with aldosterone while light labelled cells were as control.

LC-MS/MS sample preparation and running conditions. 1 mg lysates from each biological replicate (light and heavy combined) were reduced, alkylated, pre-digested by lys-c, followed by trypsin digestion overnight. Peptides were then desalted and fractionated offline into 7 fractions using Oasis PRiME HLB columns (Waters) under high pH. Elution solution used for the 7 fractions are 3% ACN, 5% ACN, 7.5% ACN, 10% ACN, 12.5% ACN, 15% ACN and 50% ACN in 0.1% trimethylamine. The phosphopeptides from each fraction were enriched using home-made TiO_2 columns (GL Science). Samples were analyzed by Thermo EASY nLC 1000 coupled with QExactive, through an EASY-Spray nano-electrospray ion source. Peptides were trapped by a pre-column (Acclaim PepMap 100, 75um*2cm, nanoviper fitting, C18, 3um, 100Å, Thermo Scientific) and analyzed by an analytical column (EASY-Spray column PepMap, 75um*25cm, nanoviper fitting, C18, 3um, 100 Å, Thermo Scientific). Buffer A was 0.1% FA and Buffer B was 100% ACN/0.1% FA. A 60 min gradient of 0-35% B was used for peptide separation. The MS was set up as full scan (m/z 300-1700) at the resolution of 70,000; 10 data dependent MS/MS scans at the

resolution of 17,500; HCD collision energy, 29%; dynamic exclusion time 30s; charge state exclusion, less than +1 and above +8. Phospho-enriched samples were run in duplicates/triplicates and flowthrough samples (total protein) were run only once per sample.

LC-MS/MS data analysis. Proteome Discoverer (version 1.4, Thermo Scientific) database searching used both SEQUEST and MASCOT against a mouse protein database (mouse.protein.v20180126.fasta, Uniprot). The parameters for Proteome Discoverer were: precursor mass tolerance, 10 ppm; fragment mass tolerance, 0.02 Da; maximum miss cleavage, 2; static modification, cysteine carbamidomethylation; variable modification: N-terminal acetylation, methionine oxidation, 10+ for heavy arginine, 6+ for heavy lysine, phosphorylation of STY. Percolator was used to calculate false discovery rate (FDR); phosphoRS 3.0 algorithm was used to evaluate phosphorylation site probability score. Only rank 1 and high confidence (with a target false discovery rate (FDR) q-value below 0.01) peptides were included in the final results. The quantification of each unique peptide was obtained from the sum of raw values from different peptide charge states, different fractions and different technical replicates. The heavy-to-light ratio of each unique peptide was calculated from the summed raw intensities of heavy or light peptide from different charge states and different fractions. Quantification ratios were normalized based on median $\log_2$ ratios of each biological replicate. Normalization was done using all peptides, including phosphopeptides and non-phosphopeptides. Phosphopeptides identified and quantified in at least three replicates were subjected to Benjamini-Hochberg (BH) FDR analysis, and those that passed the 10% BH-FDR threshold plus a few phosphopeptides with LOG2 ratios all higher than 0.75 or all lower than -0.75 were retained for further

analysis. The mass spectrometry proteomics data have been deposited to the ProteomeXchange Consortium via the PRIDE [12] partner repository with the dataset identifier PXD010032 (Username: reviewer12098@ebi.ac.uk Password: HS8uC5pG). Total proteome and identified phosphosites can be viewed from http://interpretdb.au.dk/database/mpkDCT_acute_Aldo/mpkDCT_proteome.html or http://interpretdb.au.dk/database/mpkDCT_acute_Aldo/Phosphosite.html.

Bioinformatics. Regulated phosphorylation motifs were predicted using standard settings in MotifX (http://motif-x.med.harvard.edu/motif-x.html). Go-term analysis was carried out using app ClueGo v2.5.1 in Cytoscape. Proteins (uniprot accessions used) with significant changes in phosphorylation levels were subjected for phosphorylation core analysis using Ingenuity Pathway Analysis (IPA, Qiagen) to generate functional pathways. Both direct and indirect relationships were considered in the analysis. Molecules per network was set to 140, and networks per analysis was set to 10. Confidence was set to experimentally observed.

***Statistics*.** Immunoblotting and second messenger data are expressed as mean ± S.E.M. For two groups, data meeting the statistical assumptions of normality were assessed using an unpaired Student's *t*-test. Comparisons of more than two groups were performed using a one-way ANOVA followed by Tukey's multiple comparison tests. Significance was considered at $P < 0.05$.

Associated References

1 Pedersen, N. B., Hofmeister, M. V., Rosenbaek, L. L., Nielsen, J. & Fenton, R. A. Vasopressin induces phosphorylation of the thiazide-sensitive sodium chloride cotransporter in the distal convoluted tubule. *Kidney international* **78**, 160-169, doi:10.1038/ki.2010.130 (2010).

2 Cheng, L., Wu, Q., Kortenoeven, M. L., Pisitkun, T. & Fenton, R. A. A Systems Level Analysis of Vasopressin-mediated Signaling Networks in Kidney Distal Convoluted Tubule Cells. *Sci Rep* **5**, 12829, doi:10.1038/srep12829 (2015).

3 Peng, K. C. *et al.* Tissue and cell distribution of the multidrug resistance-associated protein (MRP) in mouse intestine and kidney. *The journal of histochemistry and cytochemistry : official journal of the Histochemistry Society* **47**, 757-768 (1999).

4 Brandish, P. E., Hill, L. A., Zheng, W. & Scolnick, E. M. Scintillation proximity assay of inositol phosphates in cell extracts: high-throughput measurement of G-protein-coupled receptor activation. *Analytical biochemistry* **313**, 311-318 (2003).

5 Wu, Q. *et al.* CHIP Regulates Aquaporin-2 Quality Control and Body Water Homeostasis. *Journal of the American Society of Nephrology : JASN*, doi:10.1681/ASN.2017050526 (2017).

6 Moeller, H. B., Knepper, M. A. & Fenton, R. A. Serine 269 phosphorylated aquaporin-2 is targeted to the apical membrane of collecting duct principal cells. *Kidney international* **75**, 295-303, doi:10.1038/ki.2008.505 (2009).

7 Rosenbaek, L. L., Kortenoeven, M. L., Aroankins, T. S. & Fenton, R. A. Phosphorylation decreases ubiquitylation of the thiazide-sensitive cotransporter NCC and subsequent clathrin-mediated endocytosis. *The Journal of biological chemistry* **289**, 13347-13361, doi:10.1074/jbc.M113.543710 (2014).

8 Meyer, A. H., Katona, I., Blatow, M., Rozov, A. & Monyer, H. In vivo labeling of parvalbumin-positive interneurons and analysis of electrical coupling in identified neurons. *J Neurosci* **22**, 7055-7064, doi:20026742 (2002).

9 Poulsen, S. B. *et al.* Role of adenylyl cyclase 6 in the development of lithium-induced nephrogenic diabetes insipidus. *JCI Insight* **2**, e91042, doi:10.1172/jci.insight.91042 (2017).

10 Martensson, U. E. *et al.* Deletion of the G protein-coupled receptor 30 impairs glucose tolerance, reduces bone growth, increases blood pressure, and eliminates estradiol-stimulated insulin release in female mice. *Endocrinology* **150**, 687-698, doi:10.1210/en.2008-0623 (2009).

11 Windahl, S. H. *et al.* The role of the G protein-coupled receptor GPR30 in the effects of estrogen in ovariectomized mice. *Am J Physiol Endocrinol Metab* **296**, E490-496, doi:10.1152/ajpendo.90691.2008 (2009).

12 Vizcaino, J. A. *et al.* 2016 update of the PRIDE database and its related tools. *Nucleic acids research* **44**, D447-456, doi:10.1093/nar/gkv1145 (2016).

Additional information Table S1 and Table S2

Table S1 uploaded excel file

Table S1_mpkDCT-proteome.xlxs

(http://interpretdb.au.dk/database/mpkDCT_acute_Aldo/mpkDCT_proteome.html)

Table S2 uploaded excel file

Table S2_mpkDCT-phosphoproteome.xlxs

(http://interpretdb.au.dk/database/mpkDCT_acute_Aldo/Phosphosite.html)